Polymer Testing 98 (2021) 107189

Contents lists available at ScienceDirect

Polymer Testing

journal homepage: http://www.elsevier.com/locate/polytest

Effect of fiber attrition, particle characteristics and interfacial adhesion on the properties of PP/sugarcane bagasse fiber composites

András Bartos [a,b,*], Judit Kócs [a,b], Juliana Anggono [c], János Móczó [a,b], Béla Pukánszky [a,b]

[a] Laboratory of Plastics and Rubber Technology, Department of Physical Chemistry and Materials Science, Budapest University of Technology and Economics, H-1521, Budapest, P.O. Box 91, Hungary
[b] Institute of Materials and Environmental Chemistry, Research Centre for Natural Sciences, Eötvös Loránd Research Network, H-1519 Budapest, P.O. Box 286, Hungary
[c] Department of Mechanical Engineering, Petra Christian University, Jalan Siwalankerto 121-131, Surabaya, 60236, Indonesia

ARTICLE INFO

Keywords:
PP homopolymer
Fiber attrition
Interfacial adhesion
Acoustic emission
Fiber fracture

ABSTRACT

PP/sugarcane bagasse fiber composites were prepared by injection molding from two fractions of fibers with different particle characteristics. The mechanical properties of the composites were characterized by tensile and impact measurements, while local deformation processes by acoustic emission testing and microscopy. The determination of fiber dimensions after processing showed that considerable attrition takes place during melt processing in both the length and the diameter of the fibers. Interfacial adhesion can be improved considerably by coupling. The strength of adhesion was estimated quantitatively and adhesion was ten times stronger (1600 mJ/m^2) in the presence of the coupling agent than without it (140 mJ/m^2) leading to larger composite strength in the former case. Local deformation processes also change with the strength of adhesion, debonding dominates without the coupling agent, while fiber fracture takes place at good adhesion. Fiber fracture consumes energy that leads to an increase in impact resistance. The size of the fibers must be reduced in order to achieve better properties, but the application of coupling cannot be avoided even in that case.

1. Introduction

Polypropylene (PP) is a commodity polymer with versatile properties, which can be modified further in various ways. Because of its versatility, the growth rate of its production and use is one of the largest even among the commodity polymers [1]. It has balanced properties, good stiffness and strength, low density, reasonable price, but its impact resistance is not sufficient for certain applications. PP is often used in structural applications, especially in the automotive industry and construction, where even its stiffness must be increased [2,3]. Polymers are often reinforced with fibers of various lengths [4–9]. Recently, traditional glass and carbon fibers are frequently replaced by natural fibers or wood flour [10–14]. Besides coming from renewable resources, such fibers have several advantages: their environmental impact is very advantageous, they are strong and light at the same time and their price is low [13–15]. Another advantage of natural fibers is that they can be obtained from local sources as a side product or waste and their value-added application may help the local economy. Unfortunately, natural fibers have some drawbacks as well, their properties change with location, the time of the harvest and weather conditions, they absorb moisture, they are sensitive to temperature during processing and their adhesion to the matrix is often quite weak [15].

The properties of polymers reinforced with natural fibers are determined by several factors including component properties, composition, structure and interfacial interactions [16]. The most important characteristics of the fibers, besides their inherent strength, are their dimensions, i.e. length, diameter and aspect ratio [17,18]. Wood particles, for example, are large and thick and their aspect ratio is relatively small. Large diameter usually leads to easy debonding, the separation of the matrix and the fiber, and thus to premature failure [19]. Small aspect ratio, on the other hand, results in limited reinforcement. The dimensions of both traditional and natural fibers change during the processing of composite materials by traditional thermoplastic technologies as homogenization, injection molding or extrusion [20–23]. The attrition of the fibers has a considerable impact on reinforcement and the overall properties of the composites generally.

Fiber dimensions and attrition are analyzed thoroughly only in very few papers dealing with natural fiber-reinforced polymers [21,22,24,

* Corresponding author. Laboratory of Plastics and Rubber Technology, Department of Physical Chemistry and Materials Science, Budapest University of Technology and Economics, H-1521 Budapest, P.O. Box 91, Hungary.
E-mail address: bartos.andras@vbk.bme.hu (A. Bartos).

https://doi.org/10.1016/j.polymertesting.2021.107189
Received 20 December 2020; Received in revised form 4 March 2021; Accepted 2 April 2021
Available online 8 April 2021

25]. Often even the original dimensions of the fibers are not reported, but their change during processing is frequently neglected. According to Vázquez et al. [21] the final length of the fibers decreased to less than half of its original value in PP/bagasse fiber composites, while a much smaller change was observed by Jiménez and coworkers [22] in similar composites. Possible changes in the diameter of the fibers during processing were not measured or even considered in either case.

The other important factor determining composite properties is interfacial adhesion [26–28]. The strength of adhesion varies in a wide range depending on the chemical character of the components. Strong adhesion develops between poly (lactic acid) and natural fibers, because of the formation of hydrogen bonds [28]. Such bonds cannot form in PP, only weak van der Waals forces can develop between the matrix and the fiber. Consequently, the debonding of larger particles or fibers is very easy and properties, especially strength, deteriorate with increasing fiber content [19,29]. In order to compensate for weak interactions, various surface modifications or coupling are used in fiber-reinforced polymer composites [30–32]. In PP/natural fiber composites the most frequently applied coupling agent is maleated polypropylene (MAPP), a polymer grafted with maleic anhydride, but various small molecular weight compounds as silanes, isocyanates, and other reactive compounds [21,22,29,33–40] are also used for surface modification.

Some kind of modification is frequently used also in PP/sugarcane bagasse fiber composites because of the large size of bagasse fibers and their poor adhesion to the matrix. Luz et al. [36] found that the adhesion between PP and bagasse fibers is poor. Several groups used various treatments to improve adhesion among others an isocyanate [21], acrylic acid [21], sulfuric acid [37], alkali treatment [21,38,39] and a MAPP coupling agent [22,37,40]. The stiffness of the composites increased occasionally after the treatment [37], but usually larger improvement was achieved in strength [22,38,40].

In fiber-reinforced polymer composites frequently local deformation processes take place which are related to the fibers [28,41,42]. Such processes can be the debonding or pullout of the fiber, fiber fracture perpendicular or parallel with the fiber axis, buckling, but also the shear yielding or cavitation of the matrix can be initiated by the presence of the reinforcement. These local processes also depend very strongly on the particle characteristics of the reinforcement and on interfacial adhesion. Large size and weak interaction facilitate debonding and the latter also fiber pullout. Fiber fracture occurs more frequently in the case of strong interfacial adhesion, and the number of such events increases upon coupling [19,40]. Accordingly, the study of the effect of particle characteristics and interfacial adhesion on the processes taking place during the deformation of natural fiber-reinforced composites is crucial for the optimization of properties.

Considering the facts discussed above, the goal of this study was to prepare composites from a locally derived natural reinforcement, sugarcane bagasse fiber available in large quantities in Indonesia, and a PP homopolymer and to study the effect of fiber dimensions and interfacial adhesion on composite properties. The fibers were separated into two fractions, a short and a long fraction, and interfacial adhesion was improved by the use of a maleated PP coupling agent. Fiber characteristics were determined before and after processing to obtain information about attrition. Local deformation processes were followed by acoustic emission testing and characteristic quantities derived from the test were related to composite properties. The relevance of the results for practice is briefly discussed in the final section of the paper.

2. Experimental

2.1. Materials

The bagasse fibers were obtained directly from the sugar mill (Candi Baru Sugar Factory, Sidoarjo, Indonesia). They were washed with ethanol, dried, cut and sieved. The fibers were separated into two, a long and a short fractions in order to study the effect of fiber characteristics on composite properties. The long fraction was obtained by combining fibers collected from the 0.8 mm (20 mesh) and 0.35 mm (45 mesh) sieves, and the short fraction consisted of the fibers passing through all sieves. The dimensions of the fibers were determined by digital optical microscopy before and after processing; the characteristics are compiled in Table 1.

The polypropylene used as matrix for the composites was the Tipplen H 649 FH grade homopolymer produced by the MOL Group Ltd., Hungary. The polymer has a nominal density of 0.9 g/cm^3 and a melt flow rate of 2.5 g/10 min at 230 °C and 2.16 kg load. A polypropylene functionalized with maleic anhydride was used as coupling agent. The Scona TPPP 2112 FA grade maleated PP (MAPP) was supplied by Byk-Chemie GmbH, Germany, and it had a melt flow rate of 2–7 g/10 min at 190 °C and 2.16 kg, and a maleic anhydride content of 0.9–1.2 wt% according to the datasheet of the producer. The fiber content of the composites changed from 0 to 30 wt% in 5 wt% steps. The ratio of MAPP/fiber was 0.1 calculated for the weight of the fiber and added on the expense of the matrix polymer in all composites.

2.2. Sample preparation

The fibers and the polymer were homogenized in a twin-screw compounder (Brabender DSK 42/7, Brabender GmbH, Duisburg, Germany) at the set temperatures of 170–180-185-190 °C, and at 40 rpm. The fibers were dried before extrusion at 105 °C for 4 h in an air circulating oven (Memmert UF450, Memmert GmbH, Schwabach, Germany). Extrusion was repeated once in order to increase homogeneity. The granulated composites were injection molded into standard (ISO 527 1A) tensile bars of 4 mm thickness using a Demag IntElect 50/330-100 machine (Demag Ergotech GmbH, Schwaig, Germany). Processing parameters were 40–170-180-185-190 °C set temperatures, 300–700 bar injection pressure, 50 bar back pressure, 50 mm/s injection speed, 25 s holding time, and 30 s cooling time. The temperature of the mold was set to 40 °C. The specimens were stored at ambient temperature (25 °C, 50% RH) for a week before further testing.

2.3. Characterization, measurements

The mechanical properties were characterized by tensile and impact testing. Tensile tests were carried out using an Instron 5566 universal testing machine (Instron, Norwood, MA, USA) with a gauge length of 115 mm and 5 mm/min crosshead speed. Five parallel measurements were carried out at each composition. Modulus, yield properties (yield stress and yield strain), tensile strength and elongation-at-break were derived from recorded stress vs. strain traces. Local deformation processes were followed by acoustic emission testing. Acoustic emission (AE) signals were recorded using a Sensophone AED 404 apparatus (Geréb és Társa Ltd., Budapest, Hungary). A single “a11” resonance detector with a resonance frequency of 150 kHz was attached to the center of the specimen. The threshold level of detection was set to 24 dB. Impact resistance was characterized by the notched Charpy impact strength, which was determined according to the ISO 179 standard at 23 °C with 2 mm notch depth using a 1 J hammer on ten specimens for each material. Instrumented impact testing was carried out using a Ceast Resil 5.5 instrument (Ceast spa, Pianezza, Italy) with a 4 J hammer. The

Table 1
Effect of processing on the characteristics of the bagasse fibers used. Fiber content: 16.5 vol%.

Fiber	Coupling	Processing	Length (μm)	Diameter (μm)	Aspect ratio
Short	–	before	815 ± 626	221 ± 120	3.96
	–	after	372 ± 214	160 ± 90	2.31
	+	after	354 ± 208	150 ± 72	2.50
Long	–	before	2845 ± 1260	716 ± 385	5.09
	–	after	388 ± 276	146 ± 89	2.84
	+	after	370 ± 242	141 ± 84	2.82

characteristics of the fibers, as well as the appearance of broken surfaces, were studied by scanning electron microscopy (Jeol JSM 6380 LA, Jeol Ltd., Tokyo, Japan). Micrographs were recorded on fracture surfaces created during tensile and fracture testing, respectively. In order to determine fiber dimensions after processing, composite samples were put into boiling xylene (Molar Chemicals Kft., Halásztelek, Hungary) for 8 h to dissolve the polymer. Approximately 2 g of the composite was compressed into a thin film, cut up to smaller pieces and added to 200 ml xylene. After the complete dissolution of the polymer, the suspension was filtered using a water jet pump while hot, and then the residue remaining on the filter was washed with hot xylene. Subsequently, the fibers were dried. Fiber dimensions were determined by digital optical microscopy (Keyence VHX 500, Keyence Co., Osaka, Japan). The largest (length) and smallest (diameter) dimensions of 500–600 fibers were measured using the ImagePro 10 software (Media Cybernetics, Rockville, MD, USA) both before and after processing.

3. Results and discussion

The results are discussed in several sections. The original dimensions of the fibers and the effect of processing on them are presented in the first section, followed by the discussion of the composition dependence of properties and local deformation processes. Subsequently, the strength of interfacial adhesion and its effect on reinforcement is considered, while the effect of all factors are discussed in the final section together with relevance for practice.

3.1. Fiber characteristics, effect of processing

As described in the experimental section, the fibers obtained from the sugar mill were separated into two fractions, a short and a long one. The difference in the appearance of the fibers is demonstrated well by Fig. 1. The long fraction is fiber-like indeed, while the short one seems to be a fine powder. However, a more thorough inspection reveals that even the short fraction is fiber-like, only with a slightly smaller aspect ratio. The original dimensions of the fibers are shown in the 2nd and 5th rows of Table 1. The long fibers are much larger indeed, however, not only their length but also their diameter is considerably larger than the corresponding dimensions of the short fibers. Both dimensions are approximately three times larger for the long than for the short fibers.

Table 1 clearly demonstrates the effect of processing on fiber dimensions. Two homogenization steps in the twin-screw compounder and injection molding reduced the dimensions of the fibers considerably. The decrease is especially pronounced for the long fibers, their length decreased almost to the tenth of its original value. It is interesting to note that not only the length but the diameter of the fibers also decreased during processing indicating that the fibers are split relatively easily along their axis. Increased adhesion does not have too much effect on attrition; practically the same dimensions are obtained after processing in both the presence and the absence of the MAPP coupling agent. Interestingly the final dimensions of both fractions are very similar, although the aspect ratio of the long fibers is slightly larger than that of the short fraction. Accordingly, we can expect a rather similar effect of the two fractions on the properties of the composites.

3.2. Properties

The sugarcane bagasse fibers used as reinforcement increase the stiffness of PP considerably; modulus reaches almost twice the value of the matrix polymer in the composition range studied (Fig. 2). The effect of the two fractions is quite similar as expected; the composites containing the long fraction have somewhat larger modulus because of their larger aspect ratio. Coupling has only a marginal effect on stiffness in accordance with experience showing that modulus determined at small deformations does not depend very much on the strength of interfacial adhesion [41,42].

The composition dependence of the tensile strength of PP/sugarcane

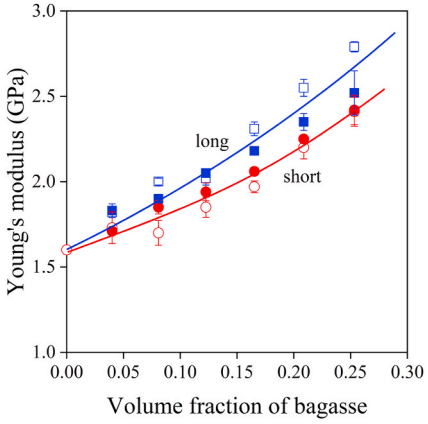

Fig. 2. Dependence of the stiffness of PP/sugarcane bagasse fiber composites on composition, initial fiber dimensions and interfacial adhesion. Symbols: (x̆,●) short fibers, (□,■) long fibers; empty symbols: without MAPP, full symbols: with MAPP.

Fig. 1. Images showing the difference in the initial dimensions of the sugarcane bagasse fibers used in the experiments; a) long fibers, b) short fibers.

bagasse fiber composites is presented in Fig. 3. The effect of the two fractions is very similar again. Strength does not change much with composition in the absence of the coupling agent; the slight increase is the result of the orientation of the fibers during injection molding [43]. Because of their small aspect ratio, the reinforcing effect of the fibers is limited. Coupling increases strength considerably due to changing local deformation processes. Increased interfacial adhesion hinders the debonding of the fibers for small and medium-sized particles. Short fibers are slightly less efficient in reinforcing the polymer probably because of their smaller length and aspect ratio. Accordingly, the identification and control of local deformation processes is crucial for the optimization of composite properties.

The dependence of the impact resistance of the composites on fiber content is somewhat surprising. Increased stiffness usually results in decreased fracture resistance for most structural materials [44], but instead of decreasing, fracture strength increases in our case (Fig. 4). Although the absolute values of impact resistance are not very large, the increase is considerable. The long fraction performs better in this case too, and coupling decreases fracture resistance somewhat. Apparently, the fibers must take part in and influence the fracture process; fibers with a larger aspect ratio are more advantageous. Unfortunately, instrumented impact testing did not reveal almost anything about the fracture process, the force vs. time traces recorded were very similar. The stress needed for crack initiation increased somewhat with increasing fiber content, but propagation energy changed only slightly. A more detailed study of the local deformation processes might offer more information about the reasons for the changes observed in the various properties of the composites as a function of the variables studied.

3.3. Local processes

Acoustic emission testing detects burst-like local processes through a piezoelectric sensor placed on the tensile specimen during the test. Such processes are the debonding of the fiber and the matrix, probably fiber pullout and the fracture of the fibers. The result of such a test is presented in Fig. 5a for the composite containing the long fraction of the fibers at 16.5 vol% in the absence of coupling. The small circles indicate individual acoustic events, while the two solid lines are the cumulative number of events vs. elongation correlation (right axis), and the stress vs. elongation trace (left axis) added for reference. The number of signals is not very large; hardly exceed 1000 during the test. The signals appear in two groups, the first at small deformations, below 1%, while the rest is scattered in the entire span of the test. The two groups indicate two processes. Previous experience shows that debonding usually occurs at

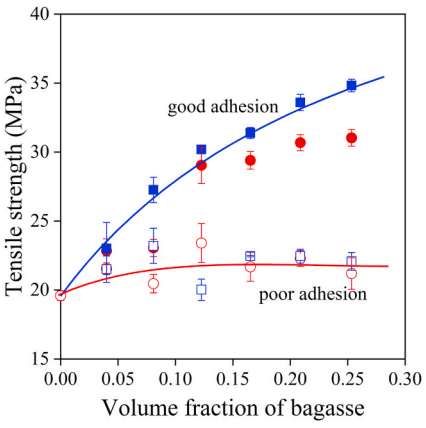

Fig. 3. Composition dependence of the tensile strength of PP/sugarcane bagasse fiber composites. Effect of interfacial adhesion. Symbols: (x̆,●) short fibers, (□,■) long fibers; empty symbols: without MAPP, full symbols: with MAPP.

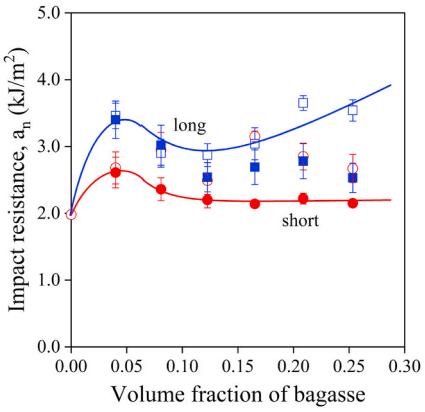

Fig. 4. Effect of fiber content on the notched Charpy impact resistance of PP/sugarcane bagasse fiber composites. Symbols: (x̆,●) short fibers, (□,■) long fibers; empty symbols: without MAPP, full symbols: with MAPP.

small deformations and stresses, while the second process might be fiber fracture and/or fiber pullout [4,19,42].

The addition of the MAPP coupling agent induces considerable changes in the acoustic emission behavior of the material (Fig. 5b). The number of signals is more than ten times larger than in the previous case and the distribution of the signals changes as well. Relatively small number of signals are detected at small deformations and much larger later in the deformation process. The majority of the signals are detected above 3% elongation. The considerable changes in the result of the test indicate that coupling and thus increased interfacial adhesion changes local processes completely and a new process becomes dominating. The identification of the actual processes is not possible based on the acoustic emission tests; they must be complemented by other methods.

Scanning electron microscopy usually offers valuable information about the mechanism of the local processes discussed above. Only two micrographs are presented in Fig. 6, because all those recorded on the fracture surface of the composites were very similar, independently of the method of creating the surface, i.e. in tensile or impact testing. Large fibers can be seen in Fig. 6a and at least two mechanisms can be identified. Debonding is clearly the dominating process taking place during deformation in the absence of the coupling agent. Some fractured fibers are also present on the surface, but we cannot determine if they were fractured during the tensile test or during the homogenization of the material. The presence of MAPP modifies the fracture surface of the composite somewhat as shown by Fig. 6b. A large fractured fiber can be located in the middle of the micrograph and other, somewhat smaller ones around it. Debonded fibers are not present on the surface practically at all. SEM micrographs support our conclusions about the mechanism of the local processes taking place around the bagasse fibers, but their unambiguous identification is difficult because of the large size of the fibers, their attrition during processing, and the rough surface of the specimens studied.

The quantitative analysis of the acoustic emission signals offers further information about local processes. Consecutive processes can be distinguished by the grouping of the individual signals and they appear as separate sections on the cumulative number of signal vs. elongation correlations. The initiation stress of the processes, called characteristic stress, can be determined by drawing straight lines to the ascending part of the correlation and then extrapolating to the horizontal axis or to the line indicating the section with lower activity in between the two groups as shown in Fig. 5a and b. These characteristic stresses are plotted against fiber content in Fig. 7. As mentioned before, two processes can be identified from the acoustic emission results at different deformations. As shown by Fig. 7, the first process occurs at the same stresses (first step) for the two fractions. The stresses in this stage are small and based on earlier experience, the related process must be the

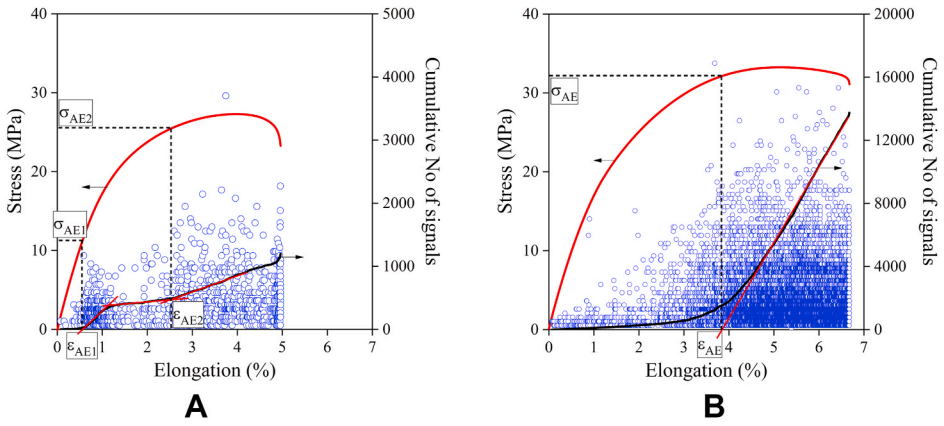

Fig. 5. Results of the acoustic emission testing of PP/sugarcane bagasse composites; (x̂) individual acoustic emission signals, the full lines are the cumulative number of signal vs. elongation (right axis) and the stress vs. elongation correlation (left axis), respectively, the latter plotted as a reference. Fiber content: 16.5 vol%; a) without MAPP, b) with the MAPP coupling agent.

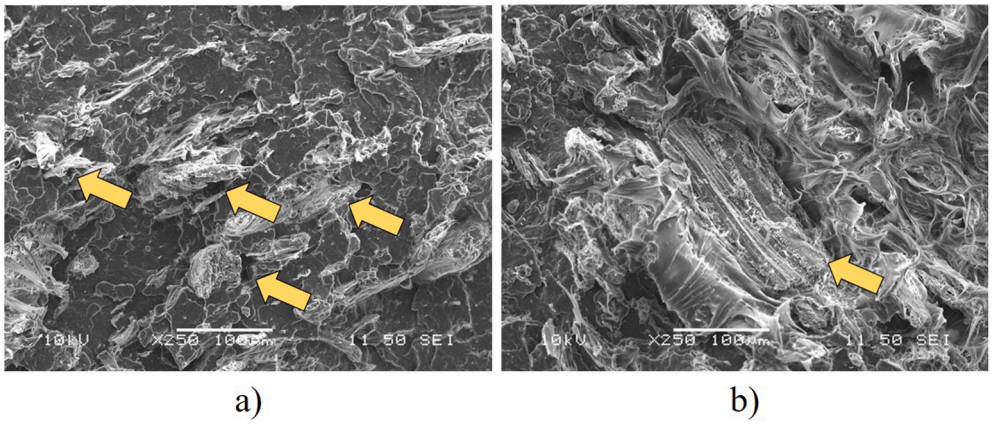

Fig. 6. SEM micrographs recorded on the fracture surface of PP/sugarcane bagasse fiber composites. The surfaces were created in tensile testing. Resulting morphology from local processes are indicated by arrows. Fiber content: 16.5 vol%. a) without coupling, b) with MAPP.

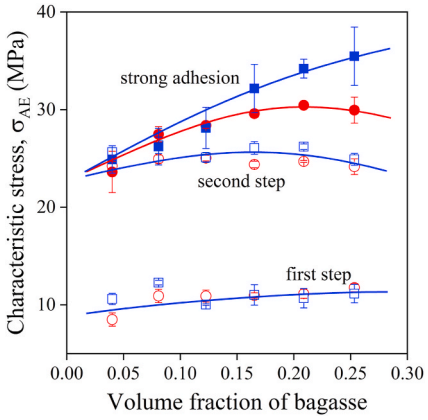

Fig. 7. Composition dependence of the characteristic (initiation) stresses of the local processes taking place around the fibers as determined by acoustic emission testing. Symbols: (x̂,●) short fibers, (□,■) long fibers; empty symbols: without MAPP, full symbols: with MAPP.

debonding of the fibers. The fibers with the largest diameter debond first and thus not aspect ratio or average size, but the size and number of thick fibers determine the initiation stress of this process. The mechanism of the second process is more difficult to identify. We saw in Table 1 that the attrition of the fibers is considerable during processing, the fibers split along their axis as well and they do this independently of the presence or absence of the coupling agent, i.e. adhesion. We may assume therefore that the second process is the fracture of the fibers along their axis. In the absence of the coupling agent only the fibers with the largest diameter fracture, since they contain more flaws than smaller ones, but the number of these events is small. The stress needed for fracture is smaller than in the other cases (second step, lowest correlation). At strong adhesion, debonding is less probable, smaller fibers also fracture, initiation stress increases. The difference between the two fractions can be assigned to the somewhat smaller diameter and larger aspect ratio of the long fraction. Accordingly, fiber dimensions, but especially interfacial adhesion have a crucial impact on local processes and thus on the properties of the composites.

3.4. Interfacial adhesion

As the results presented above show, interfacial interactions are crucial in the determination of the mechanism of local processes and the properties of the composites. However, we assumed, and changes in composite properties confirmed, that the MAPP coupling agent increases adhesion, but we do not know the extent of this increase. Using appropriate models makes possible the quantitative estimation of the change in interfacial adhesion. A model describing the composition dependence of tensile yield stress or tensile strength allows the determination of the load-bearing capacity of the reinforcing fibers [45]. The model can be expressed as

$$\sigma_T = \sigma_{T0}\,\lambda^n\,\frac{1-\phi_f}{1+2.5\,\phi_f}\exp(B\,\phi_f) \quad (1)$$

where σ_T and σ_{T0} are the true tensile strength of the composite and the matrix, respectively, ϕ_f is the volume fraction of the fiber in the composite, B expresses load-bearing capacity and it depends, among others, on interfacial adhesion. In the equation true tensile strength ($\sigma_T = \sigma\lambda$, $\lambda = L/L_0$, relative elongation) accounts for the change in specimen cross-section and λ^n for strain hardening occurring with increasing elongation. n characterizes the strain hardening tendency of the polymer and can be determined from matrix properties. The rearrangement of the equation leads to the reduced tensile strength and if we plot the natural logarithm of this latter against composition, we should obtain straight lines, the slope of which expresses the reinforcing effect of the fibers quantitatively [42]. The model was fitted to the experimental data in the way suggested and the load-bearing capacity of the fibers, i.e. reinforcement (parameter B) was calculated for the four sets of composites. The intersection of the straight lines gives the calculated strength of the matrix (σ_{T0}), while R^2, the determination coefficient, offers information about the goodness of the fit. The results are collected in Table 2 and they correspond to our expectation, interfacial adhesion improves reinforcement and the load-bearing capacity of the fibers considerably.

Although we obtained quantitative information about the effect of coupling on the reinforcing effect of the fibers by applying the model expressed in Eq. (1), direct values on adhesion are still missing. The use of another model offers a way to obtain such values. Debonding stress depends on the stiffness of the matrix (E), on the size of the particles (R) and on interfacial adhesion (F_a) in the following way

$$\sigma^D = -C_1\,\sigma^T + C_2\left(\frac{E\,F_a}{R}\right)^{1/2} \quad (2)$$

where σ^D and σ^T are debonding and thermal stresses, respectively, and C_1 and C_2 are constants, which depend on the geometry of the debonding process [46]. Debonding stress (σ^D) can be determined from acoustic emission testing (initiation stress) and if we know the constants C_1 and C_2, we can calculate adhesion strength. The constants have been determined earlier ($C_1 = 0.23 \pm 0.08$ and $C_2 = 4.31 \pm 0.5$) [47] and thus F_a was calculated for all four sets of composites. The values are listed in the third column of Table 2 and they show that the strength of adhesion increased by an order of magnitude as the result of the addition of MAPP. The large change in adhesion strength explains the modification of the mechanism of local deformation processes, the fracture of large fibers and the considerable increase in composite strength.

3.5. Discussion

The results presented in Table 1 showed that considerable fiber attrition took place during the homogenization and processing of the composites. As expected, attrition was more severe for longer and larger fibers than for smaller ones. Because of attrition, the dimensions of the fibers in the composites were very similar in spite of their largely differing initial values. Accordingly, small differences could be detected in the effect of the two fractions used and we obtained only limited information on the effect of fiber dimensions on composite properties.

Table 2
Characteristics related to interfacial adhesion; strength of adhesion (F_a) and load-bearing capacity (B).

Fiber	Coupling	F_a (mJ/m^2)[a]	σ_{T0} (MPa)	Parameter B	R^2[b]
Short	–	141	20.9	3.39	0.9678
	+	1604	21.0	4.95	0.9775
Long	–	138	20.9	3.44	0.9668
	+	1650	21.5	5.30	0.9795

a) F_a was determined on composites containing 16.5 vol% bagasse.
b) determination coefficient indicating the goodness of the fit.

On the other hand, the quantitative determination of values related to interfacial adhesion proved that interactions change drastically upon the addition of the MAPP coupling agent. Changing adhesion led to an increase of composite strength and modified local processes significantly. The role of local processes in the determination of the overall properties of composites, except stiffness, has been shown several times [4,41,42]. In order to confirm this relationship, tensile strength was plotted against the characteristic stresses determined by acoustic emission. The correlation is presented in Fig. 8. Points representing the two processes are separated from each other clearly. The characteristic stress of the first process is small and it is not related to tensile strength. The second process, on the other hand, is closely related to the strength of the composite indicating that the occurrence of the process results in the immediate failure of the material. Accordingly, the control of the local process allows the adjustment of composite strength and one way to do this is the modification of interfacial adhesion, i.e. coupling.

The last issue remaining open is the increase of impact resistance in the presence of the fibers, which is interesting from both the theoretical and the practical points of view. Increasing stiffness predicts decreasing impact resistance, thus the fibers must initiate processes, which consume energy during fracture. The most probable processes are the shear yielding of the matrix or the fracture of the fibers. Debonding leads to the formation of voids that changes the stress distribution around the fibers and often results in local yielding. However, shear yielding was not detected on any of the micrographs recorded on the fracture surface of the composites, thus we must assume that the fracture of the bagasse fibers is the process resulting in the increase of impact resistance. This phenomenon was observed earlier for large wood particles [39]. Nevertheless, we can conclude that the use of sugar cane bagasse fibers has numerous benefits. In the case of good adhesion, the stiffness and strength of PP increase considerably, and its impact resistance improves in some extent as well. The limited information obtained on the effect of fiber dimensions on properties indicates that their modification or even optimization may lead to further improvement in composite characteristics.

4. Conclusions

Considerable attrition occurs during the processing of sugar cane bagasse fibers. The larger the dimensions of the fibers the larger the extent of attrition. Although the initial dimensions of the two fiber fractions used in these experiments differed significantly, their size in the composites was very similar. Interfacial adhesion is poor in PP/bagasse fiber composites, but it can be improved by coupling. The

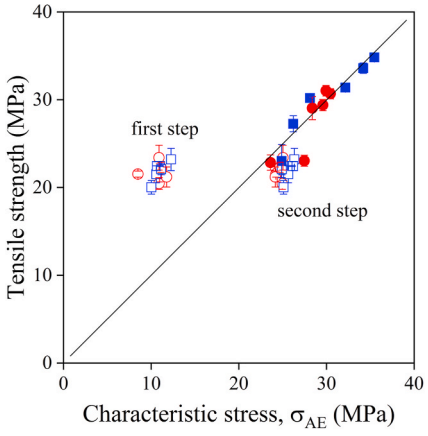

Fig. 8. Correlation between the tensile strength of the PP/bagasse fiber composites and the characteristic stresses of the local processes determined by acoustic emission testing. Symbols: (x̆,●) short fibers, (□,■) long fibers; empty symbols: without MAPP, full symbols: with MAPP.

strength of adhesion was estimated quantitatively and adhesion was ten times as strong (1600 mJ/m^2) in the presence of the coupling agent than without it (140 mJ/m^2). Consequently, the load-bearing capacity of the fibers was also very different leading to much larger tensile strength in the presence of the coupling agent. Local deformation processes also change with the strength of adhesion, debonding dominates in the absence of the coupling agent, while fiber fracture is more important at good adhesion. Fiber fracture consumes energy that leads to the increase of impact resistance upon the addition of the fibers, although the absolute value of impact strength remains relatively small (4 kJ/m^2). The overall properties of the PP composites prepared with sugarcane bagasse fibers are relatively good and probably they can be further improved by optimization. The very large size of the fibers used in these experiments is not advantageous, they must be reduced in order to achieve better properties, but even in that case, the application of coupling cannot be avoided.

Credit authorship contribution

András Bartos (Methodology, Investigation, Data curation, Writing – original draft, Writing – review & editing; Visualization); Judit Kócs (Investigation); Juliana Anggono (Conceptualization, Writing – review & editing); János Móczó; (Conceptualization, Methodology, Data curation, Writing – original draft; Writing – review & editing); Béla Pukánszky (Conceptualization, Methodology, Writing – original draft, Supervision)

Data availability statement

The raw/processed data required to reproduce these findings cannot be shared at this time as the data also form the part of an ongoing study.

Declaration of competing interest

The authors declare that they have no known competing financial interests or personal relationships that could have appeared to influence the work reported in this paper.

Acknowledgements

The National Research, Development and Innovation Fund of Hungary (OTKA K 120039 and FK 129270) is greatly acknowledged for the financial support of the research. We are also grateful to the Ministry of Research, Technology and Higher Education of the Republic of Indonesia for the research grant 002/SP2H/LT/MONO/L7/2019. The Candi Baru Sugar Factory, Indonesia is acknowledged for providing the sugarcane bagasse fibers. One of the authors (AB) is grateful also to the Pro Progressio Foundation for its support.

Appendix A. Supplementary data

Supplementary data to this article can be found online at https://doi.org/10.1016/j.polymertesting.2021.107189.

References

[1] J. Karger-Kocsis, T. Bárány, Polypropylene Handbook: Morphology, Blends and Composites, Springer International Publishing, Cham, 2019.
[2] A. Güneri, Polymers in Construction, Rapra Technology Limited, Shrewsbury, 2005.
[3] B. Flowers, Automotive applications for polypropylene and polypropylene composites, in: H. Karian (Ed.), Handbook of Polypropylene and Polypropylene Composites, Revised and Expanded, CRC Press, Boca Raton, 2003, pp. 578–586.
[4] R. Várdai, M. Ferdinánd, T. Lummerstorfer, C. Pretschuh, M. Jerabek, M. Gahleitner, G. Faludi, J. Móczó, B. Pukánszky, Effect of various organic fibers on the stiffness, strength and impact resistance of polypropylene; a comparison, Polym. Int. 70 (2021) 145–153, https://doi.org/10.1002/pi.6105.
[5] D. Kada, A. Koubaa, G. Tabak, S. Migneault, B. Garnier, A. Boudenne, Tensile properties, thermal conductivity, and thermal stability of short carbon fiber reinforced polypropylene composites, Polym. Compos. 39 (2018) E664–E670, https://doi.org/10.1002/pc.24093.
[6] E.M. Fernandes, V.M. Correlo, J.F. Mano, R.L. Reis, Polypropylene-based cork-polymer composites: processing parameters and properties, Compos. B Eng. 66 (2014) 210–223, https://doi.org/10.1016/j.compositesb.2014.05.019.
[7] A.K. Bledzki, P. Franciszczak, A. Mamun, The utilization of biochemically modified microfibers from grain by-products as reinforcement for polypropylene biocomposite, Express Polym. Lett. 8 (2014) 767–778, https://doi.org/10.3144/expresspolymlett.2014.79.
[8] J. Zhang, W. He, Y. Wu, N. Wang, X. Chen, J. Guo, The evolution of morphology, crystallization and static and dynamic mechanical properties of long glass-fibre–reinforced polypropylene composites under thermo-oxidative ageing, J Thermoplast Compos 32 (2019) 544–557, https://doi.org/10.1177/0892705718772872.
[9] J.L. Thomason, The influence of fibre length and concentration on the properties of glass fibre reinforced polypropylene: 7. Interface strength and fibre strain in injection moulded long fibre PP at high fibre content, Compos. Part A-Appl. S. 38 (2007) 210–216, https://doi.org/10.1016/j.compositesa.2006.01.007.
[10] J.L. Thomason, J.L. Rudeiros-Fernández, A review of the impact performance of natural fiber thermoplastic composites, Front. Mater. 5 (2018), https://doi.org/10.3389/fmats.2018.00060. Article 60.
[11] K.L. Pickering, M.G.A. Efendy, T.M. Le, A review of recent developments in natural fibre composites and their mechanical performance, Compos Part A-Appl S 83 (2016) 98–112, https://doi.org/10.1016/j.compositesa.2015.08.038.
[12] E. Pérez, L. Famá, S.G. Pardo, M.J. Abad, C. Bernal, Tensile and fracture behaviour of PP/wood flour composites, Compos. B Eng. 43 (2012) 2795–2800, https://doi.org/10.1016/j.compositesb.2012.04.041.
[13] L. Sobczak, R.W. Lang, A. Haider, Polypropylene composites with natural fibers and wood – general mechanical property profiles, Compos. Sci. Technol. 72 (2012) 550–557, https://doi.org/10.1016/j.compscitech.2011.12.013.
[14] O. Faruk, A.K. Bledzki, H.-P. Fink, M. Sain, Biocomposites reinforced with natural fibers: 2000–2010, Prog. Polym. Sci. 37 (2012) 1552–1596, https://doi.org/10.1016/j.progpolymsci.2012.04.003.
[15] C. Clemons, Raw materials for wood-polymer composites, in: K. Oksman, M. Sain (Eds.), Wood-polymer Composites, CRC Press LLC, Boca Raton, 2008, pp. 1–22.
[16] G. Faludi, Z. Link, K. Renner, J. Móczó, B. Pukánszky, Factors determining the performance of thermoplastic polymer/wood composites; the limiting role of fiber fracture, Mater. Des. 61 (2014) 203–210, https://doi.org/10.1016/j.matdes.2014.04.052.
[17] M. Su, J. Chen, Z. Pan, X. Li, A. Xu, J. Hong, Study on the preparation and mechanical properties of injection-moulded wood-based plastics, J. Appl. Polym. Sci. 132 (2015), https://doi.org/10.1002/app.41376.
[18] A.K. Bledzki, P. Franciszczak, A. Meljon, High performance hybrid PP and PLA biocomposites reinforced with short man-made cellulose fibres and softwood flour, Compos. Part A-Appl. S. 74 (2015) 132–139, https://doi.org/10.1016/j.compositesa.2015.03.029.
[19] L. Dányádi, K. Renner, Z. Szabó, G. Nagy, J. Móczó, B. Pukánszky, Wood flour filled PP composites: adhesion, deformation, failure, Polym. Adv. Technol. 17 (2006) 967–974, https://doi.org/10.1002/pat.838.
[20] B.M. Lekube, B. Purgleitner, K. Renner, C. Burgstaller, Influence of screw configuration and processing temperature on the properties of short glass fiber reinforced polypropylene composites, Polym. Eng. Sci. 59 (2019) 1552–1559, https://doi.org/10.1002/pen.25153.
[21] A. Vázquez, V.A. Domínguez, J.M. Kenny, Bagasse fiber-polypropylene based composites, J. Thermoplast. Compos. 12 (1999) 477–497, https://doi.org/10.1177/089270579901200604.
[22] A.M. Jiménez, F.X. Espinach, L.A. Granda, M. Delgado-Aguilar, G. Quintana, P. Fullana-i-Palmer, P. Mutjè, Tensile strength assessment of injection-molded high yield sugarcane bagasse-reinforced polypropyene, Bio. Res. 11 (2016) 6346–6361, https://doi.org/10.15376/biores.11.3.6346-6361.
[23] W.J. Liu, L.T. Drzal, A.K. Mohanty, M. Misra, Influence of processing methods and fiber length on physical properties of kenaf fiber reinforced soy based biocomposites, Compos. B Eng. 38 (2007) 352–359, https://doi.org/10.1016/j.compositesb.2006.05.003.
[24] J. Prachayawarakorn, P. Ruttanabus, P. Boonsom, Effect of cotton fiber contents and lengths on properties of thermoplastic starch composites prepared from rice and waxy rice starches, J. Polym. Environ. 19 (2011) 274–282, https://doi.org/10.1007/s10924-010-0273-1.
[25] H. Peltola, B. Madsen, R. Joffe, K. Nattinen, Experimental study of fiber length and orientation in injection molded natural fiber/starch acetate composites, Ann. Mater. Sci. Eng. (2011), https://doi.org/10.1155/2011/891940.
[26] D. Maldas, B.V. Kokta, Interfacial adhesion of lignocellulosic materials in polymer composites: an overview, Compos. Interfac. 1 (1993) 87–108, https://doi.org/10.1163/156855493X00338.
[27] S.K. Nayak, S. Mohanty, S.K. Samal, Influence of interfacial adhesion on the structural and mechanical behavior of PP-banana/glass hybrid composites, Polym. Compos. 31 (2010) 1247–1257, https://doi.org/10.1002/pc.20914.
[28] G. Faludi, G. Dora, B. Imre, K. Renner, J. Móczó, B. Pukánszky, PLA/lignocellulosic fiber composites: particle characteristics, interfacial adhesion, and failure mechanism, J. Appl. Polym. Sci. 131 (2014) 39902, https://doi.org/10.1002/app.39902.
[29] R.G. Raj, B.V. Kokta, D. Maldas, C. Daneault, Use of wood fibers in thermoplastics. VII. The effect of coupling agents in polyethylene–wood fiber composites, J. Appl. Polym. Sci. 37 (1989) 1089–1103, https://doi.org/10.1002/app.1989.070370420.
[30] C. Wang, L. Chen, J. Li, S. Sun, L. Ma, G. Wu, F. Zhao, B. Jiang, Y. Huang, Enhancing the interfacial strength of carbon fiber reinforced epoxy composites by

green grafting of poly(oxypropylene) diamines, Compos. Part A-Appl. S. 99 (2017) 58–64, https://doi.org/10.1016/j.compositesa.2017.04.003.
[31] C. Wang, J. Li, J. Yu, S. Sun, X. Li, F. Xie, B. Jiang, G. Wu, F. Yu, Y. Huang, Grafting of size-controlled graphene oxide sheets onto carbon fiber for reinforcement of carbon fiber/epoxy composite interfacial strength, Compos. Part A-Appl. S. 101 (2017) 511–520, https://doi.org/10.1016/j.compositesa.2017.07.015.
[32] M. Zhao, L. Meng, L. Ma, G. Wu, F. Xie, L. Ma, W. Wang, B. Jiang, Y. Huang, Stepwise growth of melamine-based dendrimers onto carbon fibers and the effects on interfacial properties of epoxy composites, Compos. Sci. Technol. 138 (2017) 144–150, https://doi.org/10.1016/j.compscitech.2016.11.013.
[33] S. Alila, A.M. Ferraria, A.M. Botelho do Rego, S. Boufi, Controlled surface modification of cellulose fibers by amino derivatives using N,N′-carbonyldiimidazole as activator, Carbohydr. Polym. 77 (2009) 553–562, https://doi.org/10.1016/j.carbpol.2009.01.028.
[34] G. Faludi, G. Dora, K. Renner, J. Móczó, B. Pukánszky, Improving interfacial adhesion in pla/wood biocomposites, Compos. Sci. Technol. 89 (2013) 77–82, https://doi.org/10.1016/j.compscitech.2013.09.009.
[35] P. Mutje, M.E. Vallejos, J. Girones, F. Vilaseca, A. Lopez, J.P. Lopez, J.A. Mendez, Effect of maleated polypropylene as coupling agent for polypropylene composites reinforced with hemp strands, J. Appl. Polym. Sci. 102 (2006) 833–840, https://doi.org/10.1002/app.24315.
[36] S.M. Luz, A.R. Gonçalves, A.P. Del'Arco, Mechanical behavior and microstructural analysis of sugarcane bagasse fibers reinforced polypropylene composites, Compos. Part A-Appl. S. 38 (2007) 1455–1461, https://doi.org/10.1016/j.compositesa.2007.01.014.
[37] D.R. Mulinari, J.d.P. Cipriano, M.R. Capri, A.T. Brandão, Influence of surgarcane bagasse fibers with modified surface on polypropylene composites, J. Nat. Fibers 15 (2018) 174–182, https://doi.org/10.1080/15440478.2016.1266294.
[38] I.O. Oladele, I.O. Ibrahim, A.D. Akinwekomi, S.I. Talabi, Effect of mercerization on the mechanical and thermal response of hybrid bagasse fiber/CaCO3 reinforced polypropylene composites, Polym. Test. 76 (2019) 192–198, https://doi.org/10.1016/j.polymertesting.2019.03.021.
[39] M.B. Hoque, M.S. Hossain, R.A. Khan, Study on tensile, bending and water uptake properties of sugarcane bagasse fiber reinforced polypropylene based composite, J. Biomat. 3 (2019) 18–23, https://doi.org/10.11648/j.jb.20190301.13.
[40] J. Anggono, Á.E. Farkas, A. Bartos, J. Móczó, Antoni, H. Purwaningsih, B. Pukánszky, Deformation and failure of sugarcane bagasse reinforced PP, Eur. Polym. J. 112 (2019) 153–160, https://doi.org/10.1016/j.eurpolymj.2018.12.033.
[41] K. Renner, J. Móczó, B. Pukánszky, Polymer/wood composites, in: L. Nicolais, A. Borzacchiello (Eds.), Wiley Encyclopedia of Composites, John Wiley & Sons, Inc., 2011, pp. 1–19.
[42] K. Renner, C. Kenyó, J. Móczó, B. Pukánszky, Micromechanical deformation processes in PP/wood composites: particle characteristics, adhesion, mechanisms, Compos. Part A-Appl. S. 41 (2010) 1653–1661, https://doi.org/10.1016/j.compositesa.2010.08.001.
[43] A.M. Hartl, M. Jerabek, P. Freudenthaler, R.W. Lang, Orientation-dependent compression/tension asymmetry of short glass fiber reinforced polypropylene: deformation, damage and failure, Compos. Part A-Appl. S. 79 (2015) 14–22, https://doi.org/10.1016/j.compositesa.2015.08.021.
[44] W.D. Callister, D.G. Rethwisch, Materials Science and Engineering: an Introduction, John Wiley & Son, New York, 2018.
[45] B. Pukánszky, Influence of interface interaction on the ultimate tensile properties of polymer composites, Composites 21 (1990) 255–262, https://doi.org/10.1016/0010-4361(90)90240-W.
[46] B. Pukánszky, G. Vörös, Mechanism of interfacial interactions in particulate filled composites, Compos. Interfac. 1 (1993) 411–427, https://doi.org/10.1163/156855493X00266.
[47] K. Renner, J. Móczó, G. Vörös, B. Pukánszky, Quantitative determination of interfacial adhesion in composites with strong bonding, Eur. Polym. J. 46 (2010) 2000–2004, https://doi.org/10.1016/j.eurpolymj.2010.07.008.